Available online at www.sciencedirect.com
ScienceDirect
European Journal of Pharmaceutics and Biopharmaceutics 68 (2008) 352–367
European Journal of Pharmaceutics and Biopharmaceutics
www.elsevier.com/locate/ejpb

Research paper

In-silico model of skin penetration based on experimentally determined input parameters. Part I: Experimental determination of partition and diffusion coefficients

Steffi Hansen [a], Andreas Henning [a], Arne Naegel [b], Michael Heisig [b], Gabriel Wittum [b], Dirk Neumann [c], Karl-Heinz Kostka [d], Jarmila Zbytovska [e], Claus-Michael Lehr [a], Ulrich F. Schaefer [a,*]

[a] *Saarland University, Department of Biopharmaceutics and Pharmaceutical Technology, Saarbruecken, Germany*
[b] *University of Heidelberg, Simulation in Technology, Heidelberg, Germany*
[c] *Saarland University, Centre for Bioinformatics Saar, Saarbruecken, Germany*
[d] *Department of Plastic and Hand Surgery, Caritas-Hospital, Lebach, Germany*
[e] *Charles University in Prague, Faculty of Pharmacy in Hradec Králové, Czech Republic*

Received 30 January 2007; accepted in revised form 21 May 2007
Available online 29 May 2007

Abstract

Mathematical modeling of skin transport is considered a valuable alternative of in-vitro and in-vivo investigations especially considering ethical and economical questions. Mechanistic diffusion models describe skin transport by solving Fick's 2nd law of diffusion in time and space; however models relying entirely on a consistent experimental data set are missing. For a two-dimensional model membrane consisting of a biphasic stratum corneum (SC) and a homogeneous epidermal/dermal compartment (DSL) methods are presented to determine all relevant input parameters.

The data were generated for flufenamic acid (M_W 281.24 g/mol; $\log K_{Oct/H_2O}$ 4.8; pK_a 3.9) and caffeine (M_W 194.2 g/mol; $\log K_{Oct/H_2O}$ −0.083; pK_a 1.39) using female abdominal skin. $K_{lip/don}$ (lipid-donor partition coefficient) was determined in equilibration experiments with human SC lipids. $K_{cor/lip}$ (corneocyte-lipid) and $K_{DSL/lip}$ (DSL-lipid) were derived from easily available experimental data, i.e. $K_{SC/don}$ (SC-donor), $K_{lip/don}$ and $K_{SC/DSL}$ (SC-DSL) considering realistic volume fractions of the lipid and corneocyte phases. Lipid and DSL diffusion coefficients D_{lip} and D_{DSL} were calculated based on steady state flux. The corneocyte diffusion coefficient D_{cor} is not accessible experimentally and needs to be estimated by simulation.

Based on these results time-dependent stratum corneum concentration-depth profiles were simulated and compared to experimental profiles in an accompanying study.

Keywords: Partition coefficient; Diffusion coefficient; Modeling skin penetration; Tape-stripping; Flufenamic acid; Caffeine

1. Introduction

Pharmaceutical and cosmetic industries as well as governmental institutions share a common interest in skin investigation such as bioavailability studies, risk assessment of products and consumer protection among others. In-vivo studies with humans are considered the ''gold-standard''. As these are tied to ethical, analytical and economic concerns much effort has been put into developing reliable in-vitro methods preferentially using human skin. Still the high demand for human skin conflicts with an insufficient availability. Thus, animal or bioengineered skin is often used alternatively. However, large interspecies variabilities

* Corresponding author. Department of Biopharmaceutics and Pharmaceutical Technology, Saarland University, D-66123 Saarbruecken, Germany. Tel.: +49 681 302 2019; fax: +49 681 302 4677.
E-mail address: ufs@mx.uni-saarland.de (U.F. Schaefer).

0939-6411/$ - see front matter © 2007 Elsevier B.V. All rights reserved.
doi:10.1016/j.ejpb.2007.05.012

Nomenclature

Definitions are given for the symbols used in the main text in alphabetical order

c_0	initial concentration of substance within the incubation solution
c_{exSC}	concentration within the bottom layer of the stratum corneum, i.e. the last pool of tape-strips
c_{inDSL}	concentration within the topmost layer of the viable deeper skin layers, i.e. the first pool of cryo-cuts
cor	corneocytes
D	apparent diffusion coefficient
dc/dx	concentration gradient
D_{cor}	apparent diffusion coefficient through the corneocytes
D_{DSL}	apparent diffusion coefficient through the viable deeper skin layers
Der	dermis
D_{lip}	apparent diffusion coefficient through the stratum corneum lipids
don	donor
DSL	viable deeper skin layers
Epi	epidermis
h	membrane thickness
J_{ss}	steady state flux
K	partition coefficient
$K_{cor/lip}$	partition coefficient between corneocytes and lipids
$K_{DSL/don}$	partition coefficient between viable deeper skin layers and donor
$K_{DSL/lip}$	partition coefficient between viable deeper skin layers and lipids
$K_{i/j}$	partition coefficient between skin compartment i, with i denoting SC, lip or DSL, and donor compartment j
$K_{lip/don}$	partition coefficient between lipids and donor
k_P	apparent permeability coefficient
$K_{SC/don}$	partition coefficient between stratum corneum and donor
$K_{SC/DSL}$	partition coefficient between stratum corneum and viable deeper skin layers
lip	lipids
m_0	mass of substance within the incubation solution before equilibration
m_{End}	mass of substance within the incubation solution after equilibration
m_i	dry mass of skin compartment i, with i denoting SC, lip or DSL
m_j	mass of the incubation solution
m_{Ex}	mass of substance extracted from a skin compartment
SC	stratum corneum
ϕ_{cor}	relative volume fraction of the corneocyte phase
ϕ_{lip}	relative volume fraction of the lipid phase

and insufficient barrier formation limit their significance for the situation in man.

Therefore mathematical modeling may be a potential alternative. In-silico approaches include predicting the apparent permeability coefficient k_P of various substances from easily accessible physical constants like descriptors for molecular weight, lipophilicity and solvation parameters [1–4]. Furthermore one- or two-compartmental pharmacokinetic models determine rate constants from physicochemical and physiological skin properties such as partition and diffusion coefficients, blood flow and skin thickness [5]. These allow for estimating the absolute amount present within a certain compartment after a defined time. Apart from that diffusion models additionally predict drug concentrations locally and temporally by solving the partial differential equations of Fick's 2nd law of diffusion [6]. These models describe skin penetration as a series of partition and diffusion steps which may be quantified in terms of partition coefficients K and diffusion coefficients D.

Several diffusion models with a varying degree of complexity are currently in use. Accordingly the estimation of model parameters becomes more and more challenging. The simplest cases consider a homogeneous SC such as the two-dimensional multi-layer diffusion model of Manitz et al. [7]. Here input data on $K_{SC/don}$, $K_{SC/Epi}$, $K_{Epi/Der}$, D_{don}, D_{SC} and D_{DSL} are sufficient. These are readily available for several compounds from the literature [8,9]. Subscripts indicate the respective skin layers involved in the partition or diffusion process (don, SC, lip, cor, Epi, Der and, DSL for donor, stratum corneum, intercellular stratum corneum lipids, corneocytes, epidermis, dermis and, viable deeper skin layers, i.e. viable epidermis plus dermis). More sophisticated models describe the stratum corneum geometry as "brick-and-mortar", the corneocytes being bricks and the lipids acting as intercellular mortar [10]. If only the lipoidal pathway is considered this requires input data on $K_{lip/don}$, and D_{lip} [11]. As so far partition coefficients with extracted SC lipids have only been measured for a single set of compounds several usually very similar correlations of $K_{lip/don}$ with K_{Oct/H_2O} according to a power law (linear free energy relationship) have been suggested [12–14]. Direct measurements of lateral diffusion coefficients of a small set of larger compounds (223–787 Da) and molecular oxygen in extracted SC lipids have been attempted by fluorescence recovery after photobleaching (FRAP) [15,16]. From this work also a general relationship of D_{lip} on molecular weight could be discerned. If apart from that the model allows corneocyte access it becomes crucial to break down the consecutive partition and diffusion steps experimentally according to the anatomical heterogeneity of skin. Similar to $K_{lip/don}$ Nitsche et al. related

$K_{cor/don}$ to K_{Oct/H_2O} via a power law [13]. Estimates of D_{cor} have been proposed on the basis of Phillips et al.'s analysis of hindered diffusion in media with fibrous obstacles and for the special case of water by spin-echo NMR measurements of mobile protons in guinea pig footpad SC [19,20]. Using a two-dimensional brick and mortar diffusion model with homogeneous lipid and corneocyte phases Heisig et al. were able to simulate non-steady state drug permeation through the stratum corneum [18]. Based on realistic dimensions the time resolved location of a drug within the stratum corneum was examined by systematically varying $K_{cor/lip}$, D_{lip}, and D_{cor}. An accurate resolution of the lipid channel has been attempted in [17]. The authors introduced the dimensionless parameter R to quantify the relative extents of lateral lipid diffusion and trans-bilayer hopping.

However, up to now an adequate conjunction of all these elements is missing, i.e. a brick-and-mortar diffusion model that is based on experimental input data on all relevant partition and diffusion coefficients and that is validated on the basis of experimental concentration-skin depth profiles.

Therefore, we further elaborate the model of Heisig et al. [18]. By now the model has been extended by increasing the number of corneocyte layers to 16 and adding a homogeneous epidermal/dermal compartment [21]. Thus the model membrane is composed of three different phases: corneocytes, surrounding lipids and the DSL. A graphical representation of the relevant parameters is depicted in Fig. 1. It is assumed that transport within a phase is due to Fick's second law. On the interfaces between two phases partition coefficients $K_{cor/lip}$ and K_{DSLlip} allow for an abrupt change in concentration. The flux across an interface is continuous due to mass conservation. For detailed information on model geometry, relation to measured physical quantities and applied numerical methods see the accompanying publication [21]. This study presents experimental methods and calculation techniques to determine partition and diffusion coefficients in detail as needed for the in-silico diffusion model presented in the accompanying study [21] (Table 1). Several input parameters such as $K_{lip/don}$, D_{lip} and D_{DSL} are determined experimentally.

Table 1
Overview over partition and diffusion coefficients needed for conclusive in-silico diffusion modeling of skin transport and their acquisition method

Coefficients	Direct	Derived	Source
$K_{lip/don}$	X		
$K_{cor/lip}$		X	($K_{SC/don}$; $K_{lip/don}$; Eq. (6))
$K_{DSL/lip}$		X	($K_{cor/lip}$; $K_{SC/DSL}$; Eq. (7))
D_{lip}	X		
D_{cor}		X	(D_{SC}; D_{lip}; $K_{cor/lip}$; [15])
D_{DSL}	X		

Direct parameters may be determined in experiments. Derived parameters are not directly accessible experimentally but may be determined from experimentally available data. These together with a reference of the calculation method are presented under "source".

Other parameters needed for conclusive description of skin absorption, i.e. $K_{cor/lip}$ and $K_{DSL/lip}$, cannot be measured directly and therefore are estimated from accessible experimental data. Furthermore time-dependent concentration-depth profiles through the SC and the DSL are measured. These are employed to validate the calculated drug penetration profiles in the accompanying study [21].

2. Material and methods

2.1. Material

The following materials and equipment were used: static Franz diffusion cells type 6G-01-00-15-12 (Perme Gear, Riegelsville, PA); BCA-assay kit (Sigma–Aldrich GmbH, Steinheim, Germany); dialysis membrane M_W-cut-off 12–14 kDa (Medicell International Ltd., London, Great Britain, VWR Darmstadt, Germany); Centrisart I cut-off 20 kDa (Sartorius AG, Goettingen, Germany), Durapore® membrane filters, polyvinylidene fluoride, 0.22 μm, 5 cm (Millipore, Schwalbach, Germany); Multifilm Kristallklar (Beiersdorf AG, Hamburg, Germany); cryomicrotome (HR Mark II, model 1978. SLEE, Mainz, Germany); centrifuge (Universal 30RF, Hettich Zentrifugen, Tuttlingen, Germany); freeze dryer (Alpha 2-4 LSC, Christ, Osterode, Germany); thickness meter (model 5041, type (VRZ) with

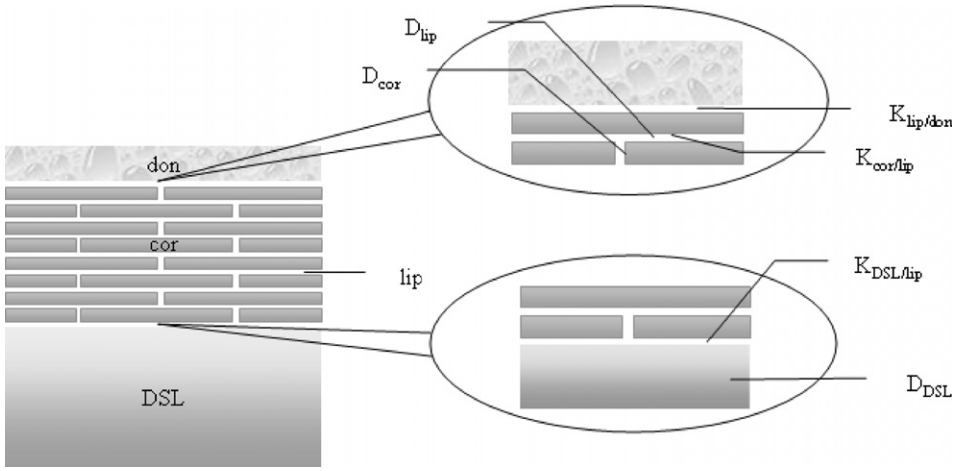

Fig. 1. Schematic picture of skin anatomy and the main partition and diffusion coefficients involved in skin transport.

tactile probe (MT) 10B; accuracy ±1 μm; Heidenhain Company, Taunreut, Germany).

2.2. Chemicals

The following chemicals were used: Flufenamic acid (M_W 281.24 g/mol; $\log K_{Oct/H_2O}$ 4.8; pK_a 3.9 [22]), caffeine (M_W 194.2 g/mol; $\log K_{Oct/H_2O}$ −0.083; pK_a 1.39 [23]), sodium chloride, potassium chloride, methanol, chloroform, trypsin type I from bovine pancreas, standard and reference lipids for HPTLC analysis: ceramide III and IV, triolein, oleic acid, cholesterol and cholesteryl oleate were provided by Sigma–Aldrich GmbH, Steinheim, Germany. Sodium azide, acetonitrile and sodium monohydrogen phosphate dihydrate were provided by Fluka Chemie AG, Buchs, Germany. Citric acid monohydrate, potassium dihydrogen phosphate, orthophosphoric acid, diethyl ether, *n*-hexane, glacial acetic acid 100%, petrolether, isopropanol, HPTLC plates, silicagel 60 non-fluorescent, copper sulphate pentahydrate were provided by Merck, Darmstadt, Germany. Keratin from bovine hoof and horn was provided by ICN biomedicals, Aurora, Ohio.

2.3. Composition of buffers

All buffer substances were of analytical grade and were prepared with purified water.

Phosphate-buffered saline (PBS) pH 7.4: 1 l contains Na_2HPO_4 1.44 g, KH_2PO_4 0.2 g, NaCl 8 g, KCl 0.2 g.

Soerensen phosphate buffer pH 7.4: 1 l contains Na_2HPO_4 9.2 g, $KH_2PO_4$2 g.

Buffer pH 2.2: 1 l contains citric acid monohydrate 20.8 g, Na_2HPO_4 0.4 g.

Buffer pH 2.6: 1 l contains orthophosphoric acid 1.16 ml, KH_2PO_4 2.04 g.

2.4. Skin samples and skin preparation techniques

Skin samples were taken from Caucasian female donors undergoing abdominal surgery with the approval of the Ethic Committee of the Caritas-Hospital Lebach, Germany. After removal of subcutaneous fatty tissue full thickness skin was stored at −26 °C for a maximum of 6 months after surgery. For details see Wagner et al. [24].

2.4.1. Preparation of stratum corneum sheets

SC sheets were prepared according to the method of Kligman [25] by two times 24 h immersion of cleaned full thickness skin pieces of approximately 12 cm^2 in 0.15% (w/v) trypsin in PBS. In between as well as afterwards the pieces were washed three times with PBS and finally freeze dried. Freeze dried membranes were kept in a freezer at −18 °C for a maximum of 6 months after surgery.

2.4.2. Preparation of corneocyte sheets

Isolated freeze dried SC sheets were delipidized with 5 ml chloroform/methanol (2:1 v/v) under occasional agitation. After 24 h delipidized membranes were removed from the extraction solution, washed three times in chloroform/methanol (2:1 v/v) and allowed to dry on air under ambient conditions.

2.4.3. Preparation of dermis sheets

Heat separation of full thickness skin was done according to Kligman [25] by 90 s immersion in water of 60 °C. The epidermis was peeled off with forceps. Leftovers only comprised of dermis.

2.5. Lipid coated membranes

SC lipids were extracted by 24 h immersion of SC in 5 ml chloroform/methanol (2:1 v/v). Organic solvents were removed in a nitrogen stream. Lipids of three donor skins (each of a surface area of roughly 60–80 cm^2) were combined, re-dissolved in chloroform/methanol (2:1 v/v) and adjusted to a final concentration of 2.5% (w/v). Durapore® membrane filters were cut into 8 approximately equal pieces (surface area per piece about 4.9 cm^2) with a scalpel and were coated by 30 times dipping into this solution. After each dip organic solvents were allowed to evaporate. Coated membranes were equilibrated at 70 °C for 10 min [26]. Filters were stored in a drying cabinet at 32 °C for 2–5 d before use as such treatment results in the lowest variability of permeability and partition data [27].

The reproducibility of the coating was ascertained by measuring the increase of thickness and mass. Membrane thickness was determined with a thickness meter equipped with a tactile probe to an accuracy of ±1 μm averaging values measured at 5 different sites (before: 114 ± 6 μm; after coating: 203 ± 23 μm). Membrane weight was determined with an analytical balance to an accuracy of ±0.01 mg (before: 15.82 ± 0.25 mg; after coating: 38.35 ± 2.77 mg).

2.6. Characterization of extracted stratum corneum lipids by WAXD

Wide angle X-ray powder diffraction data were collected at room temperature with an X'Pert PRO PRO θ-θ powder diffractometer (PANalytical, The Netherlands) with parafocusing Bragg–Brentano geometry using CuK_α radiation ($\lambda = 1.5418$ Å, $U = 40$ kV, $I = 30$ mA). Data were scanned over the angular range of 15–30° (2θ) with a Xe gas proportional detector equipped with a secondary curved monochromator. Data evaluation was performed in the software package HighScore Plus.

Lamellar spacings, d, were calculated according to $d = n\lambda/2\sin\theta$, where n is the diffraction order, λ is the wavelength of the X-ray beam and θ is the scattering angle.

2.7. Characterization of extracted stratum corneum lipids by DSC

Differential scanning calorimetry was performed using a thermal analysis data system (DSC Q100, TA Instruments,

Alzenau, Germany). The instrument was calibrated using indium as standard. Samples of 3–6 mg were heated in sealed aluminium pans from 0 to 120 °C at a scanning rate of 5 °C/min under nitrogen purge, with an empty aluminium pan as reference.

2.8. Characterization of extracted stratum corneum lipids by HPTLC

Separation and quantification of extracted SC lipids has been performed exactly as described elsewhere [28]. In short, dried and weighed extracted SC lipids were diluted with chloroform/methanol 2:1 to an appropriate degree and 1–5 μl was applied to HPTLC silica gel plates together with standard solutions (triolein and oleic acid 0.7–15 μg; sterols and ceramides 0.7–7 μg). Solvent systems and quantification methods were the same as described by Netzlaff et al. [28].

2.9. Determination of drug concentration-skin depth profiles

SC- and DSL- concentration-depth profiles were analyzed by tape-stripping of the SC and cryo-sectioning of the DSL [24]. Briefly, full thickness skin was incubated in static Franz diffusion cells with a diffusion area of 1.76 cm^2 and an acceptor volume of 12 ml at 32 ± 1 °C. Soerensen phosphate buffer pH 7.4 containing 0.05% w/v sodium azide was employed for both donor and acceptor solutions. In preliminary experiments it was ascertained that preservation with 0.05% w/v sodium azide did neither influence analytics nor penetration. Infinite dose conditions were ascertained using a donor volume of 500 μl containing 1 mg/ml of FFA or 12.5 mg/ml of caffeine. A higher donor concentration was chosen for caffeine due to analytical reasons. For both chemicals this corresponds to ≈50% of saturation concentration. In no experiment the donor concentration decreased more than 10% of the initial value. The acceptor concentration reached a maximum of 0.99% for FFA and 0.22% for caffeine of the saturation concentration (i.e. 1.97% and 0.43% of the donor concentration, respectively) after the maximum incubation time of 24 h. Thus at all times acceptor concentrations were smaller than 10% of the saturation concentration, so that perfect sink conditions were assured. After 1, 2, 6, 14 or 24 h remaining donor was removed and the surface was cleaned with dry cotton-swabs. Afterwards the skin was horizontally segmented first by tape-stripping followed by cryo-cutting according to Wagner et al. [24]. As a slight modification the first two instead of only one strip were discarded to prevent potential contamination by residual drug on the skin surface. Due to analytical reasons tape-strips were combined in pools according to the following scheme: #1+2 = discarded, #3–5 = pool 1, #6–10 = pool 2, #11–15 pool 3, # 16–20 = pool 4. Surface parallel cuts of the DSL were collected according to the following scheme: #1 = incomplete cuts, #2–5 = 4 × 25 μm sections, #6–9 = 4 × 25 μm sections, #10–11 = 2 × 25 μm sections and #12 = rest of the residual tissue.

FFA was extracted by 2 h shaking at room temperature with 0.1 N sodium hydroxide. Caffeine was extracted in a shaking water bath for 2 h at 60 °C with phosphate buffer pH 2.6 (identical to buffer used in HPLC mobile phase). Strips were extracted with 3 ml of solvent whereas 1.5 ml was used for cuts for both substances. The recovery of the extraction method is 95.35 ± 4.8.1% for FFA [24] and 87.37 ± 5.07% for caffeine.

Concentration-skin depth profiles for the SC were determined for an incubation time of 1, 2 and 6 h and for the DSL for 1, 2, 6, 14 and 24 h. For each time point and each drug three to four replicates were performed. For the SC the extract concentration is related to the SC concentration via the volume of SC removed. The SC volume per tape strip is calculated from the stripping area (1.767 cm^2) and the SC thickness per tape strip. The latter is determined microscopically via a highly standardized method [24,29]. For the DSL the extract concentration is related to the DSL concentration via weighing assuming a density of hydrated tissue of 1 g/cm^3.

The concentration of substance extracted from a pool of strips or cuts is plotted in the middle of the respective depth segment. Skin depths were calculated as given by Wagner et al. [24].

2.10. Permeation studies

Steady state flux J_{SS} of FFA and caffeine through SC, dermis or SC-lipids were measured in a separate Franz diffusion cell experiment using the respective membrane by taking samples from the acceptor compartment at time intervals of 1–36 h. Experimental conditions were as described under "Determination of drug concentration-skin depth profiles". For both compounds the donor concentration was 1 mg/ml. J_{SS} was calculated from the linear proportion of plotting the cumulative amount of substance transported per area versus time using a minimum of 5 data points according to a validated method as described in [30]. For experiments with lipid coated membrane filters it was assumed that transport is only possible via the pores of the filter (porosity = 70% of the total filter volume according to the manufacturer). Only the area of the pores (i.e. 70% of the total area) was considered for calculation of J_{ss}. Permeation experiments with uncoated filters that had been treated analogous to the coated membranes (30 times dipping in methanol/chloroform 2:1; equilibration at 70 °C for 10 min; storage at 32 °C for 2–5 d) showed no significant resistance of the filter material. This proved that the barrier is formed by the lipids.

2.11. Determination of partition coefficients by equilibration experiments

2.11.1. Decrease of donor concentration (Method 1a)

The partition coefficient $K_{i/j}$ between two phases i and j is the proportion of substance concentration [w/V] between a receiving phase i and a donating phase j [Eq. (1)].

$$K_{i/j} = \frac{c_i}{c_j} \quad (1)$$

Relating Eq. (1) to skin partition coefficients c_i and c_j are the concentrations in the respective skin compartment or the donor, respectively. Assuming a density of 1 g/cm^3 for aqueous donor, SC, cor, lip and DSL [31] the volume of the skin compartment and the donor directly translates into the mass [Eq. (2)]. Method 1a determines the concentration in the receiving skin compartment from the concentration decrease in the incubation solution where m_0 and m_{End} are the masses of substance within the incubation solution before and after equilibration; m_i is the dry mass of the respective skin compartment i.e. SC, cor, lip (i.e. the mass of lipid on the membrane filter disc) or DSL and m_j is the mass of the incubation solution.

$$K_{i/j} = \frac{(m_0 - m_{End}) \cdot m_j}{m_{End} \cdot m_i} \quad (2)$$

$K_{SC/don}$, $K_{cor/don}$, $K_{lip/don}$ and $K_{DSL/don}$ were measured based on the method introduced by Raykar et al. by equilibration experiments [32]. In contrast to Raykar et al. the original method for determining $K_{lip/don}$ was modified by coating Durapore® membrane filters with SC lipids rather than using test tube walls where they were deposited during removal of the organic solvent. The filters were prepared identically to the ones used in permeation experiments for determining D_{lip} (q.v.). This ensured setup properties like lipid organisation to be most comparable between these complementary sets of experiments. Briefly SC, delipidized SC, lipid coated filters, or prepared dermis sheets were immersed in 10 ml Soerensen buffer pH 7.4 with 0.05% w/v sodium azide containing either 10, 50, 100 or 1000 μg/ml caffeine or 10, 50 or 1000 μg/ml FFA and allowed to equilibrate at 32 °C for 24 h. Afterwards samples were drawn and analyzed for drug contents.

To exclude unspecific adsorption the test tubes and in case of $K_{lip/don}$ non-coated membrane filters were incubated with the drug solution alone. Furthermore to exclude that substances interfering with analytics are extracted by the solvent system, the membranes were soaked with the pure buffer solution for 24 h and underwent the same procedure as the drug containing solutions. All control tests proved negative.

2.11.2. Extraction of specimen (Method 1b)

The amount of substance partitioned into the respective skin compartment may further be determined directly by extraction [33,34]. The corresponding partition coefficients $K_{SC/don}$, $K_{cor/don}$, $K_{lip/don}$, and $K_{DSL/don}$ may then be calculated substituting $(m_0 - m_{End})$ in Eq. (2) by the extracted mass of substance (m_{Ex}) [Eq. (3)].

$$K_{i/j} = \frac{m_{Ex} \cdot m_j}{m_{End} \cdot m_i} \quad (3)$$

Briefly, samples were taken out of the incubation solution, washed three times in Soerensen-buffer pH 7.4 and blotted dry between filter papers. The samples were put into screw-top scintillation vials. The lids were secured with a Teflon septum. Extraction agents and conditions were the same as described for skin penetration studies. For both compounds the extraction steps were repeated until the extract concentration was below the detection limit of the HPLC.

Control samples composed either of the analyte dissolved in buffer without any skin or lipid coated filter or of the respective skin sample, or lipid coated filter immersed in pure buffer solution were subjected to an analogous procedure.

To check for completeness of extraction dried untreated or delipidized SC sheets of 2×3 cm were spiked with ethanolic solutions of FFA or caffeine (20 μl containing 5–100 μg FFA or 1–50 μg caffeine). The solvent was allowed to evaporate at ambient conditions. Samples were extracted as described above. 92–107% (w/w) FFA from untreated SC, 99–105% (w/w) FFA from corneocytes, 91–108% (w/w) caffeine from untreated SC and 93–110% (w/w) caffeine from corneocytes were recovered.

2.12. Keratin binding

Prior to the experiment water soluble low molecular weight keratin fractions resulting from the manufacturing process were removed by classical dialysis using dialysis tubing with a molecular weight cut-off of 12–14 kDa. Removal of soluble keratin fraction was considered to be complete if a BCA-assay in the supernatant performed according to the standard protocol provided by the manufacturer was negative (linear concentration range 0.2–1 mg/ml or 5–25 μg of total protein, detection limit 0.01 μg/ml). Insoluble keratin fractions were retrieved by freeze-drying.

Increasing ratios of the respective substance to keratin (0.6, 1, 10, 50, 100, 200, 300, 400, 500, 1000 μg/mg) were incubated on a magnetic stirrer (500 rpm) at 32 °C, over 24 h, i.e. until equilibration. 1.5 ml of the suspension was transferred to centrisart tubes (M_W-cut-off 20 kDa) and centrifuged for 25 min at 2795 g. The supernatant was diluted with Soerensen buffer pH 7.4 to an appropriate concentration and transferred into HPLC vials and the concentration of unbound substance was determined by HPLC. Samples containing only substance solution without keratin were subjected to the identical procedure and represented 100% free concentration.

2.13. Quantification of flufenamic acid and caffeine

Samples were analyzed by RP-HPLC using an isocratic Dionex HPLC system (Lichrospher®) RP-18 column/ 125×4 mm/5μm with a LiChroCART® 4-4 guard column (Merck-Hitachi, Darmstadt); Software: chromeleon 6.50 SP2 build 9.68.

Flufenamic acid: mobile phase: 80:20 (v/v), methanol/buffer pH 2.2; retention time: 3.5 ± 0.2 min; flow rate: 1.2 ml/min; injection volume: 50 μl; detection wavelength: 284 nm; detection limit: 15 ng/ml; quantification limit: 50 ng/ml.

Caffeine: mobile phase: 90:10 (v/v) buffer pH 2.6/acetonitrile; retention time: 5.1 ± 0.2 min; flow rate: 1.2 ml/min; injection volume: 50 µl; detection wavelength: 270 nm; detection limit: 15 ng/ml; quantification limit: 50 ng/ml.

For both compounds a calibration was performed using external standards with 0.05–25 µg/ml dissolved in Soerensen buffer pH 7.4. For extraction experiments standards were dissolved in the respective extraction fluid. If necessary, unknown samples were diluted to an appropriate concentration with the same medium as the samples prior to analysis.

2.14. Calculation of partition coefficients

2.14.1. Estimation of the stratum corneum-donor partition coefficient $K_{SC/don}$ from penetration experiments (Method 2)

The concentration-SC depth profile of a substance (i.e. $c(x,t)$ as a function of position x and time t) can be computed by using an appropriate solution to Fick's 2nd law of diffusion. Such a solution which was repeatedly applied for estimating diffusion coefficients in stratum corneum is given by Eq. (4a) "long times" [35–37]. Eq. (4a) converges rapidly for $D_{SC}\,t/h^2 > 1$.

$$c(x,t) = K_{SC/don}c_{don}\left\{1-\frac{x}{h}\right\} - \sum_{n=1}^{\infty}\frac{2}{n\pi}K_{SC/don}c_{don} \cdot \sin\left(\frac{n\pi x}{h}\right)\exp\left(\frac{-D_{SC}n^2\pi^2 t}{h^2}\right) \quad (4a)$$

Here, h is the SC thickness (FFA: 14 µm, caffeine: 15 µm), $K_{SC/don}$ is the partition coefficient between stratum corneum and donor vehicle and D_{SC} is the diffusion coefficient in the stratum corneum.

At "short times" an appropriate solution is given by Eq. (4b). For $D_{SC}t/h^2 \leqslant 1$, Eq. (4b) converges quickly and therefore is a suitable solution for Fick's 2nd law of diffusion "at short times" [38].

$$c(x,t) = K_{SC/don}c_{don}\sum_{n=0}^{\infty}\left\{\operatorname{erf}\frac{(2n+2)h+x}{2\sqrt{Dt}} - \operatorname{erf}\frac{2nh-x}{2\sqrt{Dt}}\right\} \quad (4b)$$

Both Eqs. (4a) and (4b) assume a homogeneous membrane with an infinite donor and a perfect sink below the membrane, that is the concentrations at the top and the bottom of the stratum corneum are $c(0,t) = K_{SC/don}c_{don}$ and $c(h,t) = 0\mu g/cm^3$, respectively.

The values of $K_{SC/don}$ and D_{SC} for the 1, 2 and 6 h concentration profiles of FFA and caffeine were determined in a two-step process. First, a simple grid-search was made where the diffusion coefficient D_{SC} was varied from 10^{-5} cm^2/s to 10^{-16} cm^2/s and the partition coefficient $K_{SC/don}$ from 1.0 to 300.0. For each pair of $D_{SC}/K_{SC/don}$ values the root-mean square deviation between the experimental and calculated values was computed to assess the quality of this potential solution. The best 100 results for each substance and incubation time were then subjected to a non-linear optimization routine to find the optimal values for D_{SC} and $K_{SC/don}$. This procedure assumes that D_{SC} is not a function of depth, but rather may vary with time. Thus, potential time-dependent influences of changes in the SC properties on the diffusion may be discovered and taken into account. This especially relates to swelling which is typically observed within the first hours of a Franz diffusion cell experiment when using aqueous acceptor media [24].

Due to the restrictions concerning the extraction procedure of the tape-stripping method explained under Section 2.9 only four data points along the x-axis were available for fitting. The infinite series was truncated after when the machine accuracy was reached. For example, in the case of Eq. (4b), the series was truncated when the next summand would have been less than the product of the current sum and the machine epsilon ε [39].

2.14.2. Estimation of the stratum corneum viable deeper skin layers partition coefficient $K_{SC/DSL}$ from penetration experiments

The ratio of the concentration at the bottom layer of the stratum corneum c_{exSC} (i.e. within the last pool of tape-strips) and the topmost layer of the viable epidermis c_{inDSL} (i.e. the first pool of cuts) gives $K_{SC/DSL}$ [Eq. (5)].

$$K_{SC/DSL} = \frac{c_{exSC}}{c_{inDSL}} \quad (5)$$

Using aqueous donor media the SC becomes increasingly fragile with prolonged incubation time until it finally comes off in large flaps rather than in distinct corneocyte layers. Therefore tape-stripping is only possible for incubation times up to 6 h while cryo-cutting of viable deeper skin layers is still possible after 24 h. Thus experimental data on c_{exSC} are available only up to 6 h whereas data on c_{inDSL} are also available for longer times. As c_{exSC} proved to be constant after 1 h for FFA and 2 h for caffeine no further changes of c_{exSC} are to be expected after longer incubation. For this reason the mean c_{exSC} of 1–6 h or 2–6 h was applied for calculating $K_{SC/DSL}$ for 14 and 24 h, respectively.

2.14.3. Estimation of corneocyte-lipid-and lipid-deeper skin layers partition coefficient $K_{cor/lip}$ and $K_{DSL/lip}$

By definition the (volume) concentration in the SC can be expressed using the relative volume fractions of the lipid and corneocyte phase φ_{lip} and φ_{cor}

$$c_{SC} = (\varphi_{lip} + \varphi_{cor}K_{cor/lip}) \cdot c_{lip}$$

Consequently,

$$K_{SC/don} = (\varphi_{lip} + \varphi_{cor}K_{cor/lip}) \cdot K_{lip/don}$$

holds. $K_{cor/lip}$ is estimated from $K_{SC/Donor}$ and $K_{lip/Donor}$ using Eq. (6).

$$K_{cor/lip} = \frac{1}{\varphi_{cor}} \cdot \left(\frac{K_{SC/don}}{K_{lip/don}} - \varphi_{lip}\right) \quad (6)$$

Realistic values for the volume fractions of the lipid and corneocyte phase are $\varphi_{lip} = 0.1$ and $\varphi_{cor} = 0.9$, respectively. These values result from the model geometry used for in-silico simulations and are founded empirically [21].

Analogously, $K_{DSL/lip}$ is estimated from $K_{SC/DSL}$ and $K_{cor/lip}$ Eq. (7).

$$K_{DSL/lip} = \left(\frac{\varphi_{lip} + \varphi_{cor} K_{cor/lip}}{K_{SC/DSL}}\right) \quad (7)$$

As $K_{SC/DSL}$ proved to be time dependent, only values at 24 h of incubation were considered. After 24 h $K_{SC/DSL}$ was constant for both FFA and caffeine.

2.15. Calculation of apparent diffusion coefficients

According to the steady state diffusion equation the steady state flux J_{ss} is defined as the product of the negative of the apparent diffusion coefficient D and the concentration gradient dc/dx Eq. (8). Rewriting dc/dx in Eq. (8) as the product of the initial donor concentration c_0 and the membrane-donor partition coefficient $K_{i/j}$ divided by the membrane thickness h and rearranging Eq. (8), D is calculated according to Eq. (9) [9,40].

$$J_{ss} = -D \cdot \frac{dc}{dx} \quad (8)$$

$$D = -\frac{J_{ss} h}{K_{i/j} c_0} \quad (9)$$

Substituting the variables in Eq. (9) with experimental data on J_{SS}, the values of $K_{i/j}$, c_0, and h for the respective apparent diffusion compartment (i.e. lip, DSL, SC) D_{lip}, D_{DSL} and D_{SC} were assessed. In particular D_{lip} was determined using $K_{lip/don}$ (method 1a), c_0 the donor concentration of the transport experiment, and h the thickness of the lipid coated filter (q.v.).

D_{DSL} was calculated using $K_{SC/DSL}$ after equilibration (24 h), and the concentration in the lowest SC segment c_{ExSC}. The thickness h represents the thickness of fully swollen dermis (FFA: 3.78 ± 0.27 mm, caffeine: 3.83 ± 0.47 mm; mean $\pm$ SD of 5 different sites per piece).

D_{SC} was calculated using $K_{lip/don}$ (method 1a), the initial concentration used in the transport experiment c_0, and a SC thickness h of 15 μm.

3. Results

3.1. Characterization of extracted stratum corneum lipids

3.1.1. Characterization of extracted stratum corneum lipids by WAXD

Strong reflections at spacing of 0.41 and 0.37 nm confirmed an orthorhombic lateral packing of extracted SC-lipids [41]. Concomitantly, a broad peak at about 0.4 nm spacing indicated parts of the lipids to be present in an amorphous or liquid crystalline state.

3.1.2. Characterization of extracted stratum corneum lipids by DSC

Mixtures of extracted stratum corneum lipids produced endothermic transitions at 35 ± 4 °C and 68 ± 3 °C. The blank Durapore® membrane filter showed no transitions in the inspected temperature range. Durapore® membrane filters coated with mixtures of extracted stratum corneum lipids showed an endothermic transition at 71 ± 4 °C. Due to the low mass of lipids relative to the mass of the filter the weaker transition at around 35 °C was only present in 1 of 5 samples.

3.1.3. Characterization of extracted stratum corneum lipids by HPTLC

The extracted lipid mixture was composed of $4.1 \pm 1.6\%$ cholesterol, $3.3 \pm 1.1\%$ cholesterol esters, $32.6 \pm 2.1\%$ triglycerides, $4.3 \pm 1.4\%$ free fatty acids and $4.3 \pm 1.5\%$ ceramides (total mass of lipid extracted = 100%, $n = 6$).

3.2. Keratin binding

FFA exhibits a concentration dependent keratin binding (Fig. 8). Within the observed concentration range the dependence of the bound (μg/mg keratin) versus free concentration (μg/ml) at equilibrium at 32 °C may be expressed by a Langmuir adsorption isotherm ($r^2 = 0.983$, $\chi^2 = 2.5$). The maximum mass of FFA that may be bound by 1 mg of keratin is 77.03 ± 7.81 μg. For caffeine keratin binding is negligible (Fig. 8).

3.3. Partition coefficients – directly determined values

3.3.1. $K_{SC/don}$

Equilibration experiments showed a preferred partitioning of FFA from Soerensen phosphate buffer into the SC (Table 2). Extraction (method 1b) proved the decrease of incubation solution (method 1a) to be due to a substance transfer into the SC.

$K_{SC/don}$ of FFA could further be retrieved from fitting tape-stripping profiles to Eq. (4a) (method 2, Fig. 2 and Table 3). This fit seems appropriate for the 6 h profile whereas the elevated FFA concentrations found in the lower SC layers after 1 and 2 h are represented less efficiently. Estimates of $K_{SC/don}$ are somewhat lower than values measured by equilibration experiments however, considering the well-known inter- and intra-individual variability of skin the results are still within a comparable range.

Like FFA caffeine showed a preferred partitioning from aqueous medium into the SC however, to a lesser extent (Table 2). Values measured with method 1b slightly exceed method 1a. Again $K_{SC/don}$ was also estimated from concentration-SC depth profiles (method 2) (Fig. 3 and Table 3). Estimates of method 2 excellently match results of methods 1a and 1b.

3.3.2. $K_{cor/don}$

Both FFA and caffeine preferably partition from Soerensen phosphate buffer, pH 7.4, to delipidized SC sheets (Table 2). $K_{cor/don}$ of FFA exceeds caffeine 5–7 times. For caffeine values measured with method 1b slightly, though not significantly, exceed method 1a.

Table 2
Partition coefficients of FFA and caffeine between different skin membranes (i) and phosphate buffer pH 7.4 (don) were measured by equilibration experiments and calculated from the decrease of donor concentration (method 1a, denoted as $^{*}K_{i/don}$) or from extraction (method 1b, denoted as $^{\#}K_{i/don}$)

i	FFA $^{*}K_{i/don}$	FFA $^{\#}K_{i/don}$	Caffeine $^{*}K_{i/don}$	Caffeine $^{\#}K_{i/don}$
SC	16.20 ± 4.89 ($n = 9$)	16.36 ± 3.58 ($n = 12$)	4.51 ± 2.73 ($n = 22$)	5.62 ± 0.61 ($n = 22$)
cor	n.a.	19.67 ± 7.11 ($n = 3$)	2.74 ± 1.94 ($n = 9$)	3.76 ± 0.97 ($n = 9$)
lip	20.32 ± 0.54 ($n = 4$)	23.15 ± 0.51 ($n = 4$)	2.15 ± 0.42 ($n = 4$)	n.a.
DSL	5.58 ± 0.94 ($n = 6$)	10.38 ± 2.51 ($n = 6$)	-2.22 ± 2.59 ($n = 14$)	5.10 ± 2.04 ($n = 14$)

Means ± SD, n = number of repetitions, n.a. not analyzed.

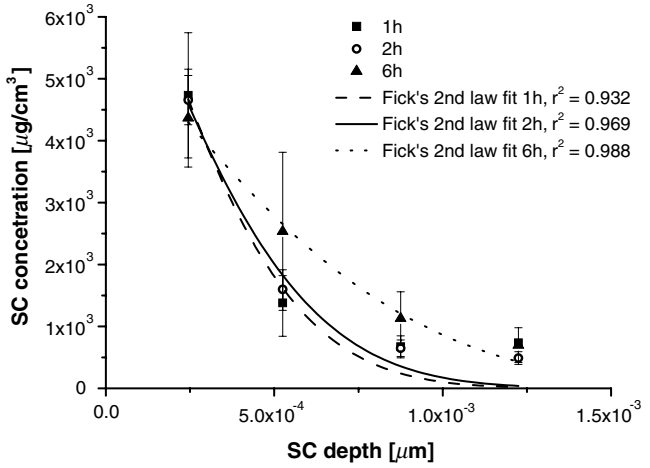

Fig. 2. Tape stripping of the SC after 1 (filled square), 2 (open circle) and 6 h (filled triangle) incubation with FFA. The concentration-SC depth profiles are fitted to Eq. (4a) (mean ± SD).

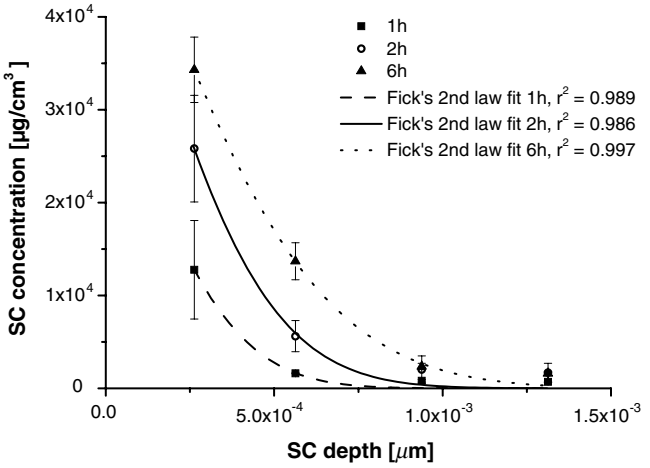

Fig. 3. Tape stripping of the SC after 1 (filled square), 2 (open circle) and 6 h (filled triangle) incubation with caffeine. The concentration-SC depth profiles are fitted to Eq. (4a) (mean ± SD).

Table 3
$K_{SC/don}$ and D_{SC} for FFA and caffeine were estimated from fitting the 1, 2 and 6 h concentration-SC depth profiles to Eq. (4a) (denoted as $^{**}K_{SC/don}$ and $^{**}D_{SC}$).

t (h)	FFA $^{**}K_{SC/don}$	FFA $^{**}D_{SC}$ (cm²/h)	Caffeine $^{**}K_{SC/don}$	Caffeine $^{**}D_{SC}$ (cm²/h)
1	9.46 ± 2.34	$7.89 \pm 3.60 * 10^{-8}$	2.92 ± 0.58	$3.97 \pm 1.06 * 10^{-8}$
2	8.12 ± 1.27	$4.75 \pm 1.44 * 10^{-8}$	4.62 ± 0.70	$2.98 \pm 0.73 * 10^{-8}$
6	5.88 ± 0.40	$3.95 \pm 0.64 * 10^{-8}$	4.70 ± 0.23	$1.82 \pm 0.17 * 10^{-8}$

Means ± SD.

3.3.3. $K_{lip/don}$

For FFA both methods 1a and 1b are in a comparable range and suggest a preferred partitioning of FFA from Soerensen phosphate buffer pH 7.4 to SC-lipids (Table 2). Caffeine also favours the lipophilic environment although $K_{lip/don}$ is only about one-tenth of FFA.

3.3.4. $K_{DSL/don}$

$K_{DSL/don}$ suggests a preferred partitioning between aqueous donor and viable skin layers for both compounds (Table 2). Incubating dermis sheets with caffeine solutions caused only non-descript concentration changes fluctuating around zero resulting in an exceptionally large standard deviation. For both compounds significantly higher amounts could be extracted from the viable skin layers than would have been estimated from the decrease of donor solution.

3.3.5. $K_{SC/DSL}$

Figs. 4 and 5 show from bottom to top the time dependency of c_{ExSC}, c_{inDSL} and $K_{SC/DSL}$ for FFA and caffeine. This allows determining $K_{SC/DSL}$ when equilibrium of partition between stratum corneum and deeper skin layers has been established. The equilibrium value of $K_{SC/DSL}$ will later be used to calculate $K_{lip/DSL}$ (q.v.). For FFA, due to constant concentrations within the bottom layer of the SC and rising concentrations at the onset of the DSL, $K_{SC/DSL}$ decreases steadily until it converges to a constant value after about 14–24 h (Fig. 4). The ratio of substance concentration of c_{ExSC} to c_{inDSL} is approximately 3:1 after 24 h.

For caffeine after initial changes of c_{ExSC} and c_{inDSL} $K_{SC/DSL}$ of caffeine levels off to a ratio of 27:1 (Fig. 5).

3.4. Partition coefficients – calculated values

3.4.1. $K_{cor/lip}$

Calculations of $K_{cor/lip}$ are based on experimental values for $K_{SC/don}$ and $K_{lip/don}$ (Table 4). $K_{SC/don}$ was acquired in 3

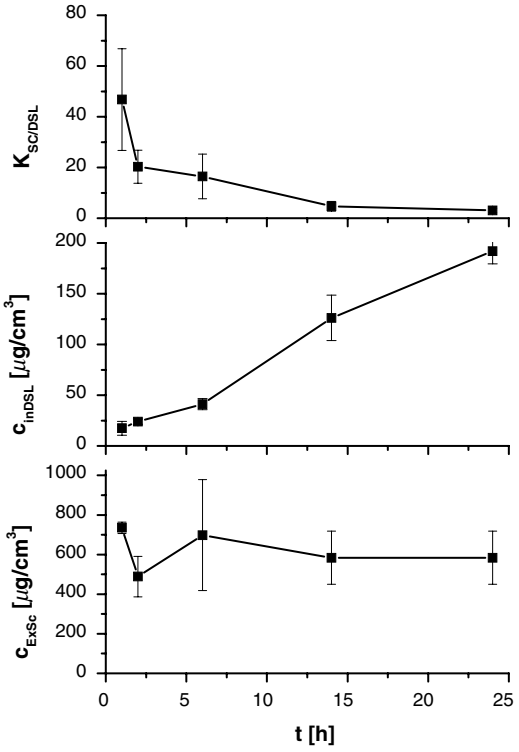

Fig. 4. FFA: Time-dependency of $K_{SC/DSL}$ (top), c_{ExSC} as analyzed by tape-stripping (down) and c_{inDSL} as analyzed by cryo-sectioning (middle) (mean ± SD).

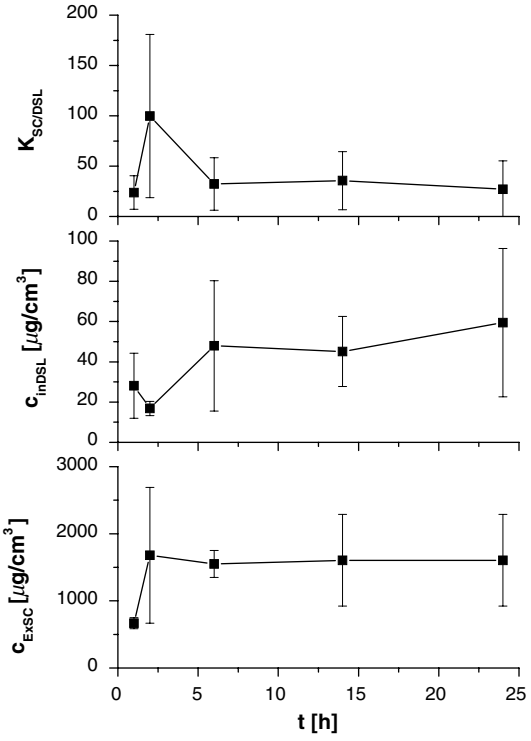

Fig. 5. Caffeine: Time-dependency of $K_{SC/DSL}$ (top), c_{ExSC} as analyzed by tape-stripping (down) and c_{inDSL} as analyzed by cryo-sectioning (middle) (mean ± SD).

Table 4
$K_{cor/lip}$ was calculated from $K_{SC/don}$ and $K_{lip/don}$ Eq. (6)

Coefficients	Source	FFA	Caffeine
$K_{cor/lip}$	$^{*}K_{SC/don}$ 1a; $^{*}K_{lip/don}$ 1a	0.77 ± 0.08	2.22 ± 1.78
	$^{**}K_{SC/don}$ 2; $^{*}K_{lip/don}$ 1a	0.21 ± 0.02	2.32 ± 0.57
$K_{DSL/lip}$	$K_{SC/DSL}$; $K_{cor/lip}$ 1a/1a	0.26 ± 0.10	0.08 ± 0.14
	$K_{SC/DSL}$; $K_{cor/lip}$ 2/1a	0.10 ± 0.04	0.08 ± 0.10

$K_{DSL/lip}$ was calculated from $K_{SC/DSL}$ and $K_{cor/lip}$ Eq. (7). The second column indicates which values were considered for calculation.

different ways. Since the results from equilibration measurements (method 1a and b, Table 2) were very similar $^{*}K_{SC/don}$ determined by method 1a was chosen for the calculation. In addition $K_{cor/lip}$ was calculated based on 6 h values of $^{**}K_{SC/don}$ as these were best represented by Eq. (4a) (Figs. 2, 3 and Table 3). Independent of the input data $K_{cor/lip}$ shows FFA to partition reluctantly from a lipophilic into a hydrophilic environment. In contrast to FFA corneocyte uptake of caffeine dominates over lipids.

3.4.2. $K_{DSL/lip}$

$K_{DSL/lip}$ suggests partitioning from SC-lipids to DSL of both FFA and caffeine to be in the same range. Both compounds prefer the lipophilic environment of the SC lipids to the more hydrophilic viable skin layers (Table 4).

3.5. Diffusion coefficients

Fig. 6a–c shows typical amount permeated per area versus time plots for FFA and caffeine. Steady state flux of FFA through mainly lipophilic compartments, i.e. SC and lipids, is ten or five times higher than that of caffeine, whereas its steady state flux through the more hydrophilic DSL is only one-tenth of caffeine (Table 5).

As expected from their similar molecular weight (see material section) usually apparent diffusion coefficients of both compounds are of the same order of magnitude within a distinct compartment and increase from SC to lipids to viable skin layers.

D_{SC} was further estimated from the decrease of $c(x,t)$ as a function of depth by fitting SC concentration-depth profiles to Eq. (4a) (Table 3). For both compounds D_{SC} decreases with time. These results range about one order of magnitude lower than values calculated on the basis of steady state flux (Table 5).

4. Discussion

Experimental data on relevant skin transport parameters of two test substances, FFA and caffeine, were collected for the validation of an advanced two-dimensional skin penetration model [21]. This included the SC- and DSL-concentration-depth-profiles, partition coefficients and diffusion coefficients. It was further sought to

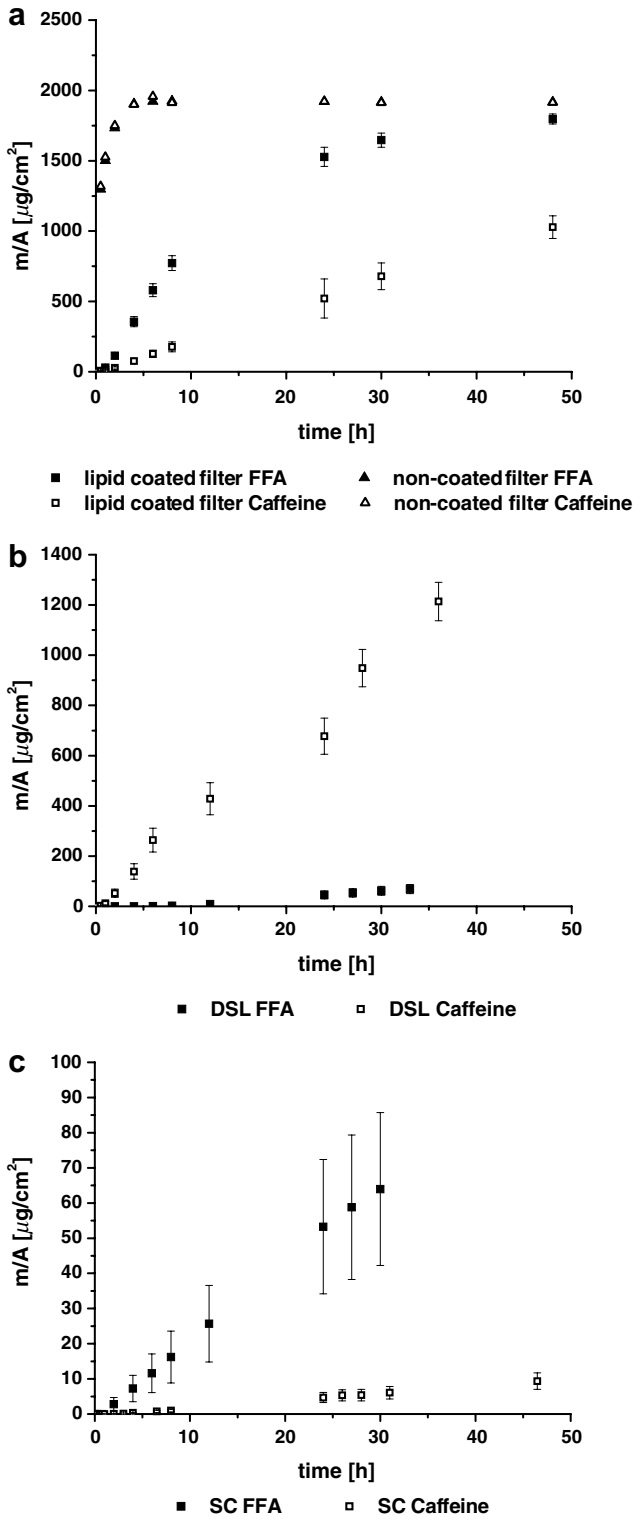

Fig. 6. Typical mass permeated per area versus time plots of FFA (closed square) and caffeine (open square) across (a) lipid coated membrane filters, (b) DSL and (c) SC. Figure 6a further includes mass permeated per area versus time plots of FFA (closed triangle) and caffeine (open triangle) across non-coated membrane filters (mean ± SD).

experimentally break down the consecutive partition and diffusion steps according to the anatomical and functional heterogeneity of the SC.

4.1. Characterization of extracted stratum corneum lipids

4.1.1. Characterization of extracted stratum corneum lipids by WAXD

The presence of orthorhombic crystalline structures showed that the lateral packing of the extracted SC lipids is representative of intact SC [41]. Together with a lamellar organisation of the SC lipid bilayers an orthorhombic lateral packing has been proposed to be crucial for the exceptional barrier properties of skin [42]. Concomitantly significant amounts of amorphous lipids were detected that might result from the fairly large amounts of triglycerides within the samples (see Section 3.1.3).

4.1.2. Characterization of extracted stratum corneum lipids by DSC

Two of the four endothermic transitions described for human SC were found. The first at around 35 °C has previously been implicated with a disordering of the lateral packing from orthorhombic to hexagonal and hexagonal to liquid crystalline phase. The second one at approximately 70 °C results from a disordering of the lamellar structure [43]. For intact stratum corneum two more transitions were reported by other authors [44]. As these result from lipids covalently attached to proteins and protein denaturation they are not to be expected in isolated skin lipids.

4.1.3. Characterization of extracted stratum corneum lipids by HPTLC

The composition of stratum corneum lipid mixtures was found to be comparable to findings of other authors. For female abdominal skin de Paepe et al. report very similar ratios of triglycerides, cholesterolesters and ceramides III and IV, as well as free fatty acid contents within the same order of magnitude [45]. The relatively larger cholesterol fraction reported by this group might be explained by age related variations. The high amounts of triglycerides are not surprising since skin originated from plastic surgery is always contaminated with triglycerides as shown by Wertz et al. [46].

4.2. Partition coefficients – directly determined values

4.2.1. $K_{SC/don}$

The uptake of substances from a topical formulation is governed by a partition process between topical formulation and uppermost skin layer, i.e. the stratum corneum. This may be quantified in terms of a partition coefficient $K_{SC/don}$. Conventionally $K_{SC/don}$ is measured by equilibration experiments where isolated SC is incubated with the respective donor formulation. In skin penetration or permeation experiments as well as in in-vivo application of drug formulations a concentration ratio identical to this partition coefficient attunes rapidly at the onset of the SC. Within the SC directly below the zone of equilibrium

Table 5
J_{ss} and D for FFA and Caffeine for SC, DSL and SC-lipids

	FFA J_{ss} (μg/cm^2/h)	FFA D (cm^2/h)	caffeine J_{ss} (μg/cm^2/h)	caffeine D (cm^2/h)
lip	108.66 ± 6.51 ($n = 4$)	$1.1 \pm 0.2 * 10^{-4}$	21.89 ± 2.0 ($n = 4$)	$2.1 \pm 0.7 * 10^{-4}$
DSL	2.50 ± 0.70 ($n = 8$)	$4.9 \pm 4.3 * 10^{-3}$	25.65 ± 4.8 ($n = 3$)	$2.3 \pm 4.0 * 10^{-3}$
SC	2.31 ± 0.96 ($n = 8$)	$1.7 \pm 0.8 * 10^{-7}$	0.21 ± 0.1 ($n = 7$)	$1.4 \pm 0.4 * 10^{-7}$

D is calculated from the steady state diffusion equation using steady state flux and the product of the concentration in the respective donating compartment (i.e. 1 mg/ml for all experiments), the partition coefficient into the membrane and the membrane thickness. (mean ± SD; n = number of repetitions.)

the substance concentration will decrease rapidly due to a concentration gradient over the membrane.

It could be shown that $K_{SC/don}$ determined by equilibration measurements may be retrieved directly from tape-stripping experiments by fitting concentration-SC depth profiles to Eq. (4a) (Table 3). For FFA this method gives slightly lower values than results from equilibration experiments (Tables 2 and 3). Customary the first one or two tape-strips are discarded due to contamination with the donor solution. Bommannan et al. identified this region to be critical for diffusion processes within the SC [47]. They investigated the SC barrier function by infrared spectroscopy and found a disorder of the SC intercellular lipids that decreases throughout the first three tape-strips and then becomes constant. Recently these findings could be transferred to in-vitro tape-stripping of skin. Mueller et al. found biphasic SC concentration-depth profiles at steady state for the diffusion of clobetasol propionate from saturated solutions containing 20% v/v propylene glycol over heat separated epidermis [48]. They attributed this behaviour to an increased corneocyte uptake or an increased intercellular solubility within the stratum corneum disjunctum [48]. This may involve a decrease of the SC diffusion coefficient in the same region causing the curvature of concentration-depth profiles to be steeper over the first three tapes than from tape four onwards. In contrast Eq. (4a) tacitly assumes constant diffusion and partition properties throughout the whole SC.

Additionally the significance of fitting the penetration data to Eq. (4a) is limited for FFA for short incubation times. Assuming perfect sink conditions at the outflow of the SC it does not represent the elevated concentration found in the lower SC after 1 and 2 h of incubation (Fig. 2). Oppositely a fit to Eq. (4a) nicely represents the 6 h profile of FFA. It seems that a so far non-specified mechanism promotes the penetration of FFA at the beginning of the diffusion process and is later compensated for by Fick'ian diffusion. It may be speculated that the special properties of FFA such as binding to keratin or its pH sensitive lipophilicity and solubility may be held responsible for this behaviour.

For caffeine estimates on $K_{SC/don}$ from SC concentration-depth profiles excellently match results of equilibration measurements (Tables 2 and 3). Caffeine does not seem to be as sensitive to depth dependent alterations in lipid fluidity within the upper SC as FFA. As the alterations of the SC ordering reported by Bommannan et al. predominantly concern the intercellular lipid channel substances using the lipid pathway should be affected more than others. This might explain why estimates of method 2 for FFA deviate from equilibration experiments while estimates for caffeine do not.

4.2.2. $K_{lip/don}$

For the in-silico model an accurate anatomical break down of partition processes was sought. As all corneocyte layers are embedded in a continuous lipid layer the boundary layer towards the donor solution is in fact lipoidal rather than cellular. Therefore $K_{lip/don}$ instead of $K_{SC/don}$ is needed to correctly describe the partitioning at the top of the SC. So far, measurements of lipid partition coefficients are only known from the original works of Raykar et al. [32]. $K_{lip/don}$ was determined in equilibration experiments employing extracted human SC-lipids brought up onto Durapore® membrane filter supports. Lipid coated membranes have previously been used by other authors in permeation studies [49–51]. Usually artificial lipid mixtures or lipids of animal origin were used. To our knowledge this is the first occasion that these were prepared completely from extracted human SC-lipids and were employed to measure partition coefficients.

4.2.3. $K_{SC/DSL}$

Especially for lipophilic substances the partition step at the interface between lipophilic SC and more hydrophilic viable epidermis/dermis may represent an additional hindrance against drug permeation. For FFA the increase in c_{inDSL} (Fig. 4, middle) may partly be explained by a water uptake into the viable skin layers during incubation in the Franz diffusion cell. This leads to a visible swelling. The increased volume of water contains additional substance. A concomitant decrease in pH from 8 to 7.4 should not impair FFA solubility (pK_a 3.9 [22]) [52]. In addition the partitioning process is superimposed by binding of FFA to viable skin layer proteins. Up to saturation of binding sites this leads to an over-proportional increase of c_{inDSL} and a concomitant decrease of $K_{SC/DSL}$ (Fig. 4, middle and top). After 24 h $K_{SC/DSL}$ then becomes constant. This value is used for calculating $K_{DSL/lip}$.

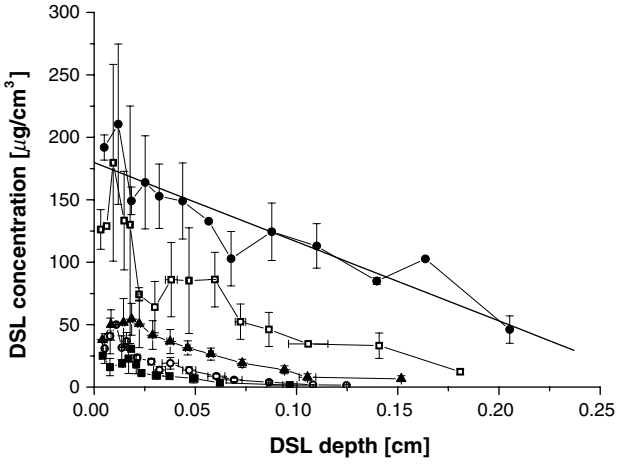

Fig. 7. Cryo-sectioning of viable deeper skin layers (DSL) after 1 (filled square), 2 (open circle), 6 (filled triangle), 14 (open square) and 24 h (filled circle) for FFA with linear regression of the 24 h graph (bold line) assuming constant membrane properties at steady state (mean ± SD).

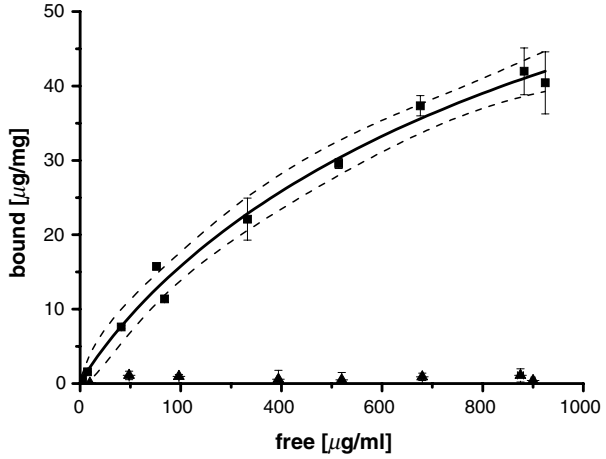

Fig. 8. The mass of substance bound per mg keratin is plotted against the equilibrium concentration of free substance within the incubation solution. Keratin binding data of FFA (filled squares) are fitted to a Langmuir-adsorption isotherm (solid line) and confidence bands (dashed lines). Caffeine binding to keratin is negligible (filled triangle) (mean ± SD).

In contrast, caffeine does not bind to proteinaceous structures (Fig. 8) and consequently shows no time dependency of c_{ExSc}, c_{inDSL} or $K_{SC/DSL}$ (Fig. 5). For the sake of consistency again the 24 h values were used to calculate $K_{DSL/lip}$.

4.3. Partition coefficients – calculated values

4.3.1. $K_{cor/lip}$

According to Eq. (6) $K_{cor/lip}$ was calculated as a secondary derived parameter employing experimental data on $K_{SC/don}$ and $K_{lip/don}$ and considering realistic relative volume fractions of the lipid and corneocyte phase, ϕ_{lip} and ϕ_{cor}.

By systematically varying ϕ_{lip} and ϕ_{cor} it can be shown that naturally occurring variations in lipid channel dimensions have only a limited impact on $K_{cor/lip}$. For example variation of ϕ_{lip} of ±20% reflects in a change of $^{*}K_{cor/lip} \pm 0.7\%$ and $^{**}K_{cor/lip} \pm 9.5\%$ for FFA and $^{*}K_{cor/lip} \pm 1.4\%$ and $^{**}K_{cor/lip} \pm 1.3\%$ for caffeine.

As recently reported by Nitsche et al. for highly lipophilic compounds, i.e. with a $\log K_{Oct/H_2O} > 5$, experimental results of $K_{SC/don}$ are largely sensitive to the lipid content and composition of the used skin samples hampering the significance of estimates of corneocyte hold-up based on $K_{SC/don}$ [13]. This problem was circumvented by determining both $K_{SC/don}$ and $K_{lip/don}$ experimentally in analogous setups using identical sets of donor skins and validated preparation techniques. One of the prerequisites of Eq. (6) is

$$K_{SC/don} = \varphi_{lip} K_{lip/don} + \varphi_{cor} K_{cor/don}$$

Substituting $K_{lip/don}$ and $K_{cor/don}$ with experimental results from equilibration measurements (method 1) a theoretical $K_{SC/don}$ may be calculated. Thus the theoretical $K_{SC/don}$ of FFA is 20.02 ± 7.68 (based on $K_{lip/don}$ and $K_{cor/don}$ determined by method 1b, i.e. extraction of skin specimen) and 2.68 ± 2.42 for caffeine (based on $K_{lip/don}$ and $K_{cor/don}$ determined by method 1a). These theoretical values of $K_{SC/don}$ are both in very good agreement with experimental results which indicates that a calculation of $K_{cor/lip}$ on this basis is valid.

Our analyses show that some degree of corneocyte uptake may be claimed for both FFA and caffeine (Table 4). In accordance with their octanol–water partition coefficients $K_{cor/lip}$ of caffeine is higher than that of FFA. It must be kept in mind that alternatively to partitioning into the corneocytes part or all of the substance could bind to proteins of the cornified envelope or to keratin. Especially FFA proved a likely candidate for protein binding whereas no binding was detected for caffeine (Fig. 8).

4.3.2. $K_{DSL/lip}$

Again an accurate anatomical break down of partition steps was sought. Therefore our method for calculating $K_{cor/lip}$ was expanded to the partition step at the interface DSL-lipid Eq. (7). According to the compound lipophilicity partitioning from SC-lipids to viable epidermis of FFA should be hampered whereas caffeine should prefer the DSL. Thus $K_{DSL/lip}$ of FFA is to be expected lower than that of caffeine. Our results suggest otherwise (Table 4). First, this mirrors the improved solubility of weak acids like FFA under moderate alkaline conditions within the DSL. Second, a high binding of FFA to proteins of the viable skin layers, such as collagen, elastin or melanin, will further raise the concentration within the DSL of this particular substance and hence will increase $K_{DSL/lip}$. This behaviour may be investigated by measuring $K_{DSL/don}$. Incubating dermis sheets with FFA led to a measurable decrease in the concentration of the incubation solution (method 1a, Table 2). Still, extracted amounts were up to two times higher than would have been estimated from analyzing the decrease of the donor concentration (method

1b, Table 2). In contrast, for caffeine no relevant decrease in concentration of the incubation solution could be detected. Still, significant amounts of caffeine were extracted from the DSL. Consequently FFA enters the DSL by partitioning or binding to proteins and also by water of hydration while caffeine will only be dissolved in water of hydration and will not bind to epidermal or dermal proteins. Third, this hints that the solubility of hydrophilic substances like caffeine in SC lipids may be much better than usually assumed.

4.4. Diffusion coefficients

4.4.1. D_{lip}

Lipid coated membranes have widely been used for diffusion measurements. In contrast to our study most of the cited experiments were performed with lipid mixtures of artificial or animal origin [50,53]. De Jager et al. could demonstrate that especially lamellar organisation and lateral packing are highly sensitive to lipid composition and manufacturing conditions [54]. This problem was circumvented by using lipids extracted from human stratum corneum. By DSC measurements it could be shown that the thermal behaviour and thus the crystallinity of the extracted stratum corneum lipids on the membrane support is very similar to the in-vivo situation. What is more WAXD measurements revealed that a significant portion of the lipids is present in an orthorhombical crystalline state. However, due to the presence of amorphous lipids and the absence of corneocytes the 3D structure of the lipids on the filters will probably be different from the in-vivo situation. Thus D_{lip} can only be an approximation. Furthermore co-extracted triglycerides might act as a possible penetration enhancer in permeation experiments [29] and thus may lead to an overemphasis of D_{SC} and D_{lip}. However, our measured values for D_{lip} queue nicely with literature data on lipid diffusion coefficients. Lange-Lieckfeldt and Lee reported that ratios ranging from 10^2–10^4 with lipid diffusion rates of 10^{-8}–10^{-9} cm^2/s result from SC geometry reflecting the tortuous diffusion pathway and the low diffusion area [53]. The ratio of $D_{\mathrm{lip}}/D_{\mathrm{SC}}$ was $6.4 * 10^2$ (D_{SC} determined according to Eq. (9)) or $1.4 * 10^4$, $2.3 * 10^4$, $2.8 * 10^4$ (D_{SC} for 1, 2 and 6 h determined according to Eq. (4a)) for FFA and $1.5 * 10^3$ (D_{SC} determined according to Eq. (9)) or $5.3 * 10^3$, $0.7 * 10^3$, $1.2 * 10^4$ (D_{SC} for 1, 2 and 6 h determined according to Eq. (4a)) for caffeine (Tables 3 and 5). This does not necessarily imply impenetrable corneocytes. They still may act as a reservoir if the rate of transport is lowest within intercellular lipids and hence determines the overall diffusion velocity through the SC.

Further, our measured values for D_{lip} are in good agreement with lateral diffusion coefficients measured with a fluorescence recovery technique in extracted stratum corneum lipids [15]. Diffusion within the plane of the lipid bilayers is believed to be considerably slower than perpendicular to it. However, Johnson et al. found lateral- but not trans-bilayer diffusion coefficients are sufficient to explain the overall resistance of solute permeation through the SC [11]. In addition it has been suggested that lipid bilayers might be oriented not strictly parallel to the corneocytes possibly allowing a continuous pathway for lateral diffusion [17].

In view of these facts it is justified to employ our measured apparent lipid diffusion coefficients as direct input data for the in-silico model presented in the accompanying paper [21]. This assumes constant diffusion properties within all lipid bilayers irrespective of the stratum corneum depth.

4.4.2. D_{DSL}

Cross et al. reported for a series of aliphatic alcohols an additional partition step between epidermis and dermis significantly influencing maximum flux and apparent permeability coefficient if compound $\log K_{\mathrm{Oct/H_2O}}$ was 2 and higher [9]. Consequently for caffeine no additional hindrance is to be expected ($\log K_{\mathrm{Oct/H_2O}} = 0.083$ [23]). Likewise may be assumed for FFA, as this is completely ionized within the fully swollen epidermis and dermis [52]. If transport is indeed homogeneous throughout the whole viable skin layers the steady state concentration gradient should be linear. Experimental data on the steady state DSL-concentration gradient are available from surface parallel segmentation of the DSL (Fig. 7). Substituting $\mathrm{d}c/\mathrm{d}x$ and $J_{\mathrm{ss\ DSL}}$ in Eq. (8) directly by experimental data it is possible to calculate D_{DSL}. For FFA linear regression of 24 h DSL-cryo-cutting data revealed a slope of the $6.34 * 10^2$ μg/cm^4 with the intercept with the y-axis at $1.80 * 10^2$ μg/cm^3 and a reasonable r^2 of 0.823. Thus D_{DSL} calculates to $3.9 * 10^{-3} \pm 1.7 * 10^{-3}$ which is very similar to estimates on the basis of J_{ssDSL}, $K_{\mathrm{SC/DSL}}$, c_{ExSC} and h_{DSL} (Table 5). Therefore diffusion properties are indeed homogeneous through the viable skin layers for FFA. Consequently our calculated values for D_{DSL} for both FFA and caffeine may be used as direct input data for mathematical modeling of skin penetration [21].

4.4.3. D_{SC}

Estimates of D_{SC} from fitting the 1, 2 and 6 h concentration-SC depth profiles to Eq. (4a) suggest a decreasing diffusion velocity with time for both FFA and caffeine. As already mentioned water uptake may impact on the SC diffusion properties. On first sight our results seem contradictory to the well-known permeation enhancing effect of water which is probably due to a disruption of intercellular SC lipids [55]. However, this effect may probably be antagonized by a concomitant increase in path length due to swelling of corneocytes. As a significant proportion of both compounds was found to partition into the corneocytes a decrease in D_{SC} seems a possible logical consequence. In contrast to D_{lip} and D_{DSL}, D_{SC} cannot be used as direct input for in-silico modeling due to the inhomogeneous character of the SC. However, the accompanying study

shows that D_{SC} together with D_{lip} and $K_{cor/lip}$ is a powerful tool to estimate D_{cor} [21].

5. Conclusion

Skin transport of drug substances from a topical formulation may be described in terms of partition and diffusion coefficients that account for abrupt changes in the environmental lipophilicity and diffusion characteristics of the medium. This study describes methods and data to measure the relevant partition and diffusion steps involved in skin transport taking into account its anatomical heterogeneity. While several coefficients such as $K_{lip/don}$, D_{lip} and D_{DSL} may be measured experimentally, others such as $K_{cor/lip}$, $K_{DSL/lip}$ and D_{cor} can only be determined indirectly. Equations are presented to calculate $K_{cor/lip}$ and $K_{DSL/lip}$ from experimentally available data. For two compounds with different physicochemical properties, i.e. flufenamic acid and caffeine, the complete data set has been collected for the case of diffusion from an aqueous donor buffered at pH 7.4 across human skin. Where available, experimental and calculated coefficients were compared to literature data and were found to be consistent.

Acknowledgements

The Deutsche Forschungsgemeinschaft (DFG Grant BIZ 4/1) and the ZEBET (Zentralstelle zur Erfassung und Bewertung von Ersatz- und Ergänzungsmethoden zum Tierversuch) are thanked for financial support. Dr. J. Maixner from the Institute of Chemical Technology, Prague, Czech Republic is acknowledged for his assistance with the X-ray diffraction measurements.

References

[1] R.O. Potts, R.H. Guy, Predicting skin permeability, Pharm. Res. 9 (1992) 663–669.
[2] W.J. Pugh, I.T. Degim, J. Hadgraft, Epidermal permeability – penetrant structure relationship. 4. QSAR of permeant diffusion across human stratum corneum in terms of molecular weight, H-bonding and electron charge, Int. J. Pharm. 197 (2000) 203–211.
[3] D. Neumann, O. Kohlbacher, C. Merkwirth, T. Lengauer, A fully computational model for predicting percutaneous drug absorption, J. Chem. Inf. Model. 46 (2006) 424–429.
[4] B.M. Magnusson, W.J. Pugh, M.S. Roberts, Simple rules defining the potential of compounds for transdermal delivery or toxicity, Pharm. Res. 21 (2004) 1047–1054.
[5] K.D. McCarley, A.L. Bunge, Pharmacokinetic models of dermal absorption, J. Pharm. Sci. 90 (2001) 1699–1719.
[6] W.J. Albery, J. Hadgraft, Percutaneous absorption: theoretical description, J. Pharm. Pharmacol. 31 (1979) 129–139.
[7] R. Manitz, W. Lucht, K. Strehmel, R. Weiner, R. Neubert, On mathematical modeling of dermal and transdermal drug delivery, J. Pharm. Sci. 87 (1998) 873–879.
[8] K. Tojo, C.C. Chiang, Y.W. Chien, Drug permeation across the skin: effect of penetrant hydrophilicity, J. Pharm. Sci. 76 (1987) 123–126.
[9] S.E. Cross, B.M. Magnusson, G. Winckle, Y. Anissimov, M.S. Roberts, Determination of the effect of lipophilicity on the in vitro permeability and tissue reservoir characteristics of topically applied solutes in human skin layers, J. Invest. Dermatol. 120 (2003) 759–764.
[10] A.S. Michaels, S.K. Chandrasekaran, J.E. Shaw, Drug permeation through human skin: theory and in vitro experimental measurement, AIChE J. 21 (1975) 985–996.
[11] M.E. Johnson, D. Blankschtein, R. Langer, Evaluation of solute permeation through the stratum corneum: lateral bilayer diffusion as the primary transport mechanism, J. Pharm. Sci. 86 (1997) 1162–1172.
[12] B.D. Anderson, W.I. Higuchi, P.V. Raykar, Heterogeneity effects on permeability – partition coefficient relationships in human stratum corneum, Pharm. Res. 5 (1988) 566–573.
[13] J.M. Nitsche, T.F. Wang, G.B. Kasting, A two-phase analysis of solute partitioning into the stratum corneum, J. Pharm. Sci. 95 (2006) 649–666.
[14] S. Mitragotri, A theoretical analysis of permeation of small hydrophobic solutes across the stratum corneum based on scaled particle theory, J. Pharm. Sci. 91 (2002) 744–752.
[15] M.E. Johnson, D.A. Berk, D. Blankschtein, D.E. Golan, R.K. Jain, R.S. Langer, Lateral diffusion of small compounds in human stratum corneum and model lipid bilayer systems, Biophys. J. 71 (1996) 2656–2668.
[16] M.E. Hatcher, W.Z. Plachy, Dioxygen diffusion in the stratum corneum: an EPR spin label study, Biochim. Biophys. Acta 1149 (1993) 73–78.
[17] T.F. Wang, G.B. Kasting, J.M. Nitsche, A multiphase microscopic diffusion model for stratum corneum permeability. I. Formulation, solution, and illustrative results for representative compounds, J. Pharm. Sci. 95 (2006) 620–648.
[18] M. Heisig, R. Lieckfeldt, G. Wittum, G. Mazurkevich, G. Lee, Non steady-state descriptions of drug permeation through stratum corneum. I. The biphasic brick-and-mortar model, Pharm. Res. 13 (1996) 421–426.
[19] K.J. Packer, T.C. Sellwood, Proton magnetic resonance studies of hydrated stratum corneum. Part 2. Self diffusion, J. Chem. Soc. Faraday Trans. II 74 (1978) 1592–1606.
[20] R.J. Phillips, W.M. Deen, J.F. Brady, Hindered transport in fibrous membranes and gels: effect of solute size and fiber configuration, J. Colloid Interf. Sci. 139 (1990) 363–373.
[21] A. Naegel, S. Hansen, D. Neumann, C.-M. Lehr, U.F. Schaefer, G. Wittum, M. Heisig, In-silico model of skin penetration based on experimentally determined input parameters. Part II: Mathematical modelling of in-vitro diffusion experiments. Identification of critical input parameters. Eur. J. Pharm. Biopharm., 68 (2008) 368–379.
[22] E. Abignente, P. de Caprariis, in: K. Florey (Ed.), Flufenamic Acid, vol. 11, Academic Press, New York, London, 1982, p. 324.
[23] M.U. Zubair, M.M.A. Hassan, I.A. Al-Meshal, in: K. Florey (Ed.), Caffeine, vol. 15, Academic Press Inc., London, 1986.
[24] H. Wagner, K.H. Kostka, C.-M. Lehr, U.F. Schaefer, Drug distribution in human skin using two different in vitro test systems: comparison with in vivo data, Pharm. Res. 17 (2000) 1475–1481.
[25] A.M. Kligman, E. Christophers, Preparation of isolated sheets of human stratum corneum, Arch. Dermatol. Res. 88 (1963) 702–705.
[26] M. de Jager, W. Groenink, J. van der Spek, C. Janmaat, G. Gooris, M. Ponec, J. Bouwstra, Preparation and characterization of a stratum corneum substitute for in vitro percutaneous penetration studies, Biochim. Biophys. Acta 1758 (2006) 636–644.
[27] E. Jaeckle, U.F. Schaefer, H. Loth, Comparison of effects of different ointment bases on the penetration of ketoprofen through heat-separated human epidermis and artificial lipid barriers, J. Pharm. Sci. 92 (2002) 1396–1406.
[28] F. Netzlaff, M. Kaca, U. Bock, E. Haltner-Ukomady, P. Meiers, C.-M. Lehr, U.F. Schaefer, Permeability of the reconstructed human epidermis model Episkin(R) comparison to various human skin preparations, Eur. J. Pharm. Biopharm., 66 (2007) 127–134.
[29] F. Theobald. In-vitro Methoden zur biopharmazeutischen Qualitätsprüfung von Dermatika unter Berücksichtigung der Lipidzusammensetzung des Stratum Corneum. Dissertation Saarbruecken (1998).

[30] M. Schaefer-Korting, U. Bock, A. Gamer, A. Haberland, E. Haltner-Ukomadu, M. Kaca, H. Kamp, M. Kietzmann, H.C. Korting, H.-U. Kraechter, C.-M. Lehr, M. Liebsch, A. Mehling, F. Netzlaff, F. Niedorf, M.K. Ruebbelke, U. Schaefer, E. Schmidt, S. Schreiber, K.-R. Schroeder, H. Spielmann, A. Vuia, Reconstructed human epidermis for skin absorption testing: Results of the German prevalidation study, Altern Lab Anim 34 (2006) 283–294.
[31] E. Jaeckle. Stratum Corneum analoge Lipidmischungen als Diffusionsmedien, ihre Eigenschaften und deren Beeinflussung durch Salbengrundlagen. Dissertation (1996).
[32] P.V. Raykar, M.-C. Fung, B.D. Anderson, The role of protein and lipid domains in the uptake of solutes by human stratum corneum, Pharm. Res. 5 (1988) 140–150.
[33] C. Surber, K.P. Wilhelm, M. Hori, H.I. Maibach, R.H. Guy, Optimization of topical therapy: partitioning of drugs into stratum corneum, Pharm. Res. 7 (1990) 1320–1324.
[34] D. van der Merwe, J.E. Riviere, Comparative studies on the effects of water, ethanol and water/ethanol mixtures on chemical partitioning into porcine stratum corneum and silastic membrane, Toxicol In Vitro 19 (2005) 69–77.
[35] J. Hadgraft, Calculations of drug release rates from controlled release devices. The slab, Int. J. Pharm. 2 (1979) 177–194.
[36] F. Pirot, Y.N. Kalia, A.L. Stinchcomb, G. Keating, A. Bunge, R.H. Guy, Characterization of the permeability barrier of human skin in vivo, Proc. Natl. Acad. Sci. USA 94 (1997) 1562–1567.
[37] C. Herkenne, A. Naik, Y.N. Kalia, J. Hadgraft, R.H. Guy, Pig ear skin ex vivo as a model for in vivo dermatopharmacokinetic studies in man, Pharm. Res. 23 (2006) 1850–1856.
[38] H.S. Carslow, J.C. Jaeger, Conduction of heat in soils, Clarendon Press, Oxford, 1959.
[39] Sun, Numerical Computation Guide, Sun Microsystems Inc., Palo Alto, 2000.
[40] S.E. Cross, W.J. Pugh, J. Hadgraft, M.S. Roberts, Probing the effect of vehicles on topical delivery: understanding the basic relationship between solvent and solute penetration using silicone membranes, Pharm. Res. 18 (2001) 999–1005.
[41] J.A. Bouwstra, G.S. Gooris, M.A. Salomons-de Vries, J.A. Van der Spek, W. Bras, Structure of human stratum corneum as a function of temperature and hydration: A wide-angle X-ray diffraction study, Int. J. Pharm. 84 (1992) 205–216.
[42] M.W. De Jager, G.S. Gooris, I.P. Dolbnya, W. Bras, M. Ponec, J.A. Bouwstra, The phase behaviour of skin lipid mixtures based on synthetic ceramides, Chem. Phys. Lipids 124 (2003) 123–134.
[43] H. Tanojo, J.A. Bouwstra, H.E. Junginger, H.E. Bodde, Thermal analysis studies on human skin and skin barrier modulation by fatty acids and propylene glycol, J. Therm. Anal. Calorim. 57 (1999) 313–322.
[44] C.L. Silva, S.C.C. Nunes, M.E.S. Eusebio, A.A.C.C. Pais, J.J.S. Sousa, Thermal behaviour of human stratum corneum: a differential scanning calorimetry study at high scanning rates, Skin Pharmacol. Physiol. 19 (2006) 132–139.
[45] K. De Paepe, A. Weerheim, E. Houben, D. Roseeuw, M. Ponec, V. Rogiers, Analysis of epidermal lipids of the healthy human skin: factors affecting the design of a control population, Skin Pharmacol. Physiol. 17 (2004) 23–30.
[46] P.W. Wertz, D.C. Swarzendruber, K.C. Madison, D.T. Downing, Composition and morphology of epidermal cyst lipids, J. Invest. Dermatol. 89 (1987) 419–425.
[47] D. Bommannan, R.O. Potts, R.H. Guy, Examination of stratum corneum barrier function in vivo by infrared spectroscopy, J. Invest. Dermatol. 95 (1990) 403–408.
[48] B. Mueller, Y.G. Anissimov, M.S. Roberts, Unexpected clobetasol propionate profile in human stratum corneum after topical application in vitro, Pharm. Res. 20 (2003) 1835–1837.
[49] W. Abraham, D.T. Downing, Preparation of model membranes for skin permeability studies using stratum corneum lipids, J. Invest. Dermatol. 93 (1989) 809–813.
[50] M. De Jager, W. Groenink, R. Bielsa I Guivernau, E. Andersson, N. Angelova, M. Ponec, J. Bouwstra, A novel in vitro percutaneous penetration model: evaluation of barrier properties with P-aminobenzoic acid and two of its derivatives, Pharm. Res. 23 (2006) 951–960.
[51] D. Kuempel, D.C. Swartzendruber, C.A. Squier, P.W. Wertz, In vitro reconstitution of stratum corneum lipid lamellae, Biochim. Biophys. Acta 1372 (1998) 135–140.
[52] H. Wagner, K.H. Kostka, C.-M. Lehr, U.F. Schaefer, pH profiles in human skin: influence of two in vitro test systems for drug delivery testing, Eur. J. Pharm. Biopharm. 55 (2003) 57–65.
[53] R. Lange-Lieckfeldt, G. Lee, Use of a model lipid matrix to demonstrate the dependence of the stratum corneum's barrier properties on its internal geometry, J. Control. Release 20 (1992) 183–194.
[54] M.W. De Jager, G.S. Gooris, I.P. Dolbnya, M. Ponec, J.A. Bouwstra, Modelling the stratum corneum lipid organisation with synthetic lipid mixtures: The importance of synthetic ceramide composition, Biochim. Biophys. Acta 1664 (2004) 132–140.
[55] L. Norlen, A. Emilson, B. Forslind, Stratum corneum swelling. Biophysical and computer assisted quantitative assessments, Arch. Dermatol. Res. 289 (1997) 506–513.